View metadata, citation and similar papers at core.ac.uk

brought to you by CORE

provided by Elsevier - Publisher Connector

Cell, Vol. 116, 51–61, January 9, 2004, Copyright ©2004 by Cell Press

Histone H3.1 and H3.3 Complexes Mediate Nucleosome Assembly Pathways Dependent or Independent of DNA Synthesis

Hideaki Tagami,[1,3,4] Dominique Ray-Gallet,[2,3] Geneviève Almouzni,[2] and Yoshihiro Nakatani[1,*]
[1]Dana-Farber Cancer Institute
and Harvard Medical School
Boston, Massachusetts 02115
[2]Section de Recherche
Institut Curie
UMR 218 du CNRS
26 Rue d'Ulm
75248 Paris Cedex 05
France

Summary

Deposition of the major histone H3 (H3.1) is coupled to DNA synthesis during DNA replication and possibly DNA repair, whereas histone variant H3.3 serves as the replacement variant for the DNA-synthesis-independent deposition pathway. To address how histones H3.1 and H3.3 are deposited into chromatin through distinct pathways, we have purified deposition machineries for these histones. The H3.1 and H3.3 complexes contain distinct histone chaperones, CAF-1 and HIRA, that we show are necessary to mediate DNA-synthesis-dependent and -independent nucleosome assembly, respectively. Notably, these complexes possess one molecule each of H3.1/H3.3 and H4, suggesting that histones H3 and H4 exist as dimeric units that are important intermediates in nucleosome formation. This finding provides new insights into possible mechanisms for maintenance of epigenetic information after chromatin duplication.

Introduction

The basic module of chromatin, the nucleosome, consists of 146 base pairs of DNA wrapped around an octamer of four core histones and exists in a variety of forms that contribute to the definition of distinct functional domains within the nucleus (Wolffe, 1998). Covalent modifications of the canonical core histones, including acetylation, phosphorylation, methylation, and monoubiquitination, are used to mark nucleosomes to create chromatin domains with a range of functions. The information encoded by the modifications can contribute to the formation and/or maintenance of transcriptionally active and inactive chromatin in response to various signaling pathways (Turner, 2000; Jenuwein and Allis, 2001). The discovery of histone variants has led to the emerging notion that these other histones could also be used to mark nucleosomes and contribute to chromatin regulation. Histone variants, also called replacement histones, were originally identified as products of histone genes whose synthesis occurs outside of S phase (Zweidler, 1984). This is in contrast with the tight regulation imposed on the synthesis of the vast majority of histones (S phase histones). Indeed, S phase histone synthesis is coupled to DNA replication in order to provide material for the bulk of nucleosome assembly when the genome is duplicated.

The critical question becomes how these variant histones are incorporated into nucleosomes during the life of the cell. Their expression both during and outside of S phase suggests that they can be deposited onto DNA at either time. In light of the fact that, to date, the most information is available concerning the control of H3–H4 deposition onto DNA, we focused our attention on variants of histone H3. In mammals, in addition to the CENP-A variants, three isotypes of histone H3 have been identified. Two of them, H3.1 and H3.2, are closely related (only differing in a Cys-Ser substitution at amino acid position 96) and belong to the family of S phase subtypes (Franklin and Zweidler, 1977). In contrast, the third one, H3.3, is expressed during S phase but also in G1, G2, and G0 stages in Chinese hamster ovary cells (Wu et al., 1982). Furthermore, H3.3 synthesis is maintained throughout differentiation, whereas the levels of H3.1 and H3.2 transcripts decrease as cell division slows down during the process of differentiation (Brown et al., 1985; Wunsch and Lough, 1987). In accordance with this observation, an increased proportion of H3.3 is detected in murine tissues that produce long-lived differentiated cells with very low rates of cell division in the adult (Zweidler, 1984). Histone H3.3 differs at 4 and 5 amino acid positions compared with H3.2 and H3.1, respectively. In all vertebrates studied so far, both H3.2 and H3.3 are expressed, yet in budding yeast only one H3 histone is expressed which is most similar to the vertebrate H3.3 variant (Baxevanis and Landsman, 1998). A recent study in *Drosophila*, using GFP-tagged H3 (closely related to mammalian H3.2) and GFP-tagged H3.3, showed that H3 is exclusively incorporated during replication whereas H3.3 can be deposited both during and outside of S phase (Ahmad and Henikoff, 2002). Furthermore, H3.3 deposition appeared to be targeted to specific loci, including active rDNA arrays, suggesting a link between its deposition and specific transcription states.

To identify the associated partners of the major and variant histone H3, we used a biochemical strategy to purify H3.1 and H3.3 complexes. We found that the purified complexes contain predeposited forms of histones H3.1/H3.3 and H4. Importantly, the H3.1 complex contains the CAF-1 histone chaperone, whereas the H3.3 complex contains the HIRA histone chaperone. Given that CAF-1 and HIRA mediate DNA-synthesis-dependent and -independent histone deposition, respectively, our data suggest mechanisms whereby major and variant histone H3 are deposited via distinct pathways. Surprisingly, we also found that histones H3 and H4 in these complexes exist as a heterodimer, suggesting that histone H3 and H4 are deposited in chromatin as a dimeric unit, rather than as a tetrameric unit. Based on these

*Correspondence: yoshihiro_nakatani@dfci.harvard.edu
[3]These authors contributed equally to this work.
[4]Present address: Division of Biological Science, Graduate School of Science, Nagoya University, Chikusa, Nagoya, Aichi 464-8602, Japan.

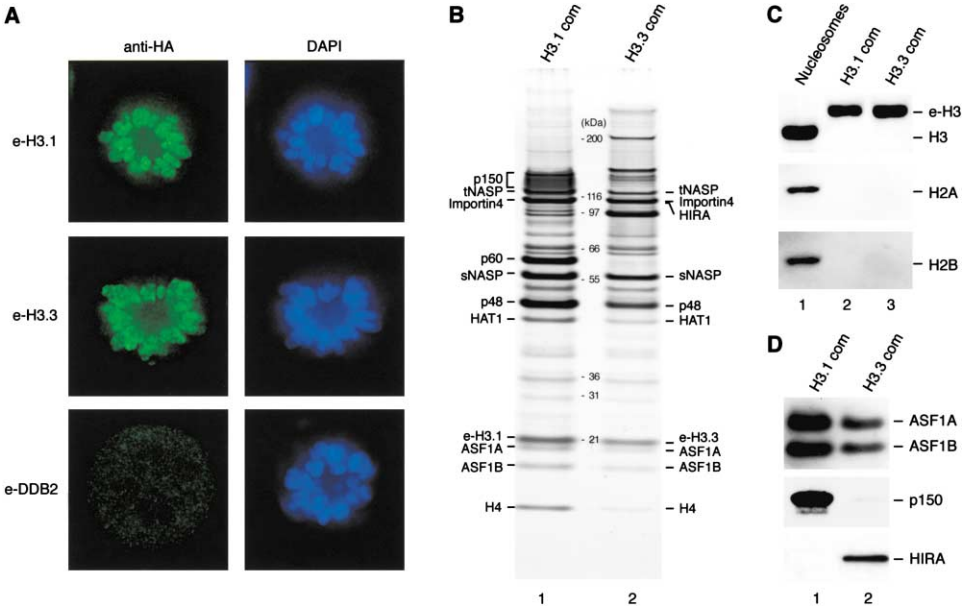

Figure 1. Identification of the H3.1 and H3.3 Complexes

(A) e-H3.1 and e-H3.3 colocalizations with mitotic chromosomes. HeLa cells expressing e-H3.1 (top), e-H3.3 (middle), and e-DDB2 (bottom) are stained with anti-HA antibody (left) and DAPI (right).

(B) Silver staining of the H3.1 and H3.3 complexes (H3.1 com and H3.3 com). The polypeptides identified by mass spectrometric analyses are indicated.

(C) The H3.1 and H3.3 complexes lack histones H2A and H2B. The H3.1 (lane 2) and H3.3 (lane 3) complexes as well as mononucleosomes purified from HeLa cells (lane 1) were analyzed by immunoblotting with antihistone H3 (top), antihistone H2A (middle), and anti-H2B (bottom) antibodies.

(D) CAF-1 p150 and HIRA are specific to the H3.1 and H3.3 complexes, respectively. The H3.1 (lane 1) and H3.3 (lane 2) complexes were analyzed by immunoblotting with anti-ASF1 (top), anti-CAF-1 p150 (middle), and anti-HIRA (bottom) antibodies.

data, we discuss mechanisms of chromatin duplication and maintenance.

Results

Purification of Predeposited Histones H3.1 and H3.3

To explore the mechanisms whereby histones H3.1 and H3.3 are deposited into chromatin, we purified these histones and their associated proteins by our immunoaffinity purification method (Nakatani and Ogryzko, 2004). Histones H3.1 and H3.3 were each stably expressed as fusion proteins with C-terminal FLAG- and HA-epitope tags (e-H3.1/e-H3.3) in HeLa cells by retroviral transduction. Immunofluorescent staining of e-H3.1 or e-H3.3 in these cells reveals that the tagged histones colocalize with mitotic chromosomes, indicating that the presence of the epitope tag does not interfere with the deposition of H3 in vivo (Figure 1A, top and middle). In control experiments, e-DDB2, the 48 kDa subunit of DDB tagged with the same epitopes and which binds to chromatin in a UV damage-dependent manner (Groisman et al., 2003), did not colocalize with mitotic chromosomes (Figure 1A, bottom). We conclude from these data that e-H3.1 and e-H3.3 are functionally deposited into nucleosomes in vivo.

To analyze predeposited forms of e-H3.1 and e-H3.3, we purified them from nuclear extracts by sequential immunoprecipitation with anti-FLAG antibody followed by anti-HA antibody. As a control, we performed mock purification from untransduced HeLa cells, which do not express epitope-tagged proteins, and detected no polypeptides by silver staining (data not shown) (Ikura et al., 2000; Ogawa et al., 2002), indicating that any polypeptides copurifying with e-H3.1 or e-H3.3 could be specific interactors. Although H3.1 and H3.3 differ by only five amino acid residues in humans, SDS-PAGE analysis of the purified complexes revealed that the subunit compositions of the histone H3.1 and H3.3 complexes are distinct (Figure 1B).

Mass spectrometric and immunoblotting analyses identified histone H4 as a common component in both the H3.1 and H3.3 complexes (Figures 1B). Although the intensity of e-H3.1/e-H3.3 staining appears to be higher than that of H4 in silver-stained gels, we observed that recombinant e-H3.1/e-H3.3 and H4 proteins loaded with equal molar absorptivities showed similar ratios of silver-staining intensities (data not shown). Thus, e-H3.1/e-H3.3 and H4 in the purified complexes could be present in stoichiometric amounts.

In contrast to their presence in nucleosomes, histones H2A and H2B were not detected in either complex (Figure 1C). Thus, the e-H3.1/e-H3.3 and H4 subunits in these complexes could represent predeposited forms of these histones.

Histone Chaperones in the H3.1 and H3.3 Complexes

Consistent with the hypothesis that the purified complexes contain predeposited histones, several known

histone chaperones (or histone binding proteins) were found in the H3.1 and H3.3 complexes. Two closely related histone chaperones, antisilencing factor 1A (ASF1A) and ASF1B, were found in both complexes (Figures 1B and 1E). ASF1 proteins have been shown to interact with histones H3 and H4 and to synergize with CAF-1 to assemble nucleosomes in a pathway coupled to DNA synthesis during replication in *Drosophila* embryo extracts (Tyler et al., 1999, 2001) or repair in human cell extracts (Mello et al., 2002). Intriguingly, the histone H1 binding protein, NASP, a human homolog of *Xenopus* N1/N2, was also a common component of both complexes (Figure 1B) (Richardson et al., 2000; Alekseev et al., 2003). A shorter form of NASP was also detected; although it is uncertain if this form corresponds to the previously reported alternatively spliced product, sNASP (Alekseev et al., 2003).

Remarkably, the entire set of CAF-1 subunits, p150, p60, and p48, was specifically identified only in the H3.1 complex (Figure 1B). Immunoblotting of the purified complexes showed that CAF-1 p150 is highly specific to the H3.1 complex (Figure 1E), supporting the view that CAF-1 is a DNA replication-dependent histone chaperone. While CAF-1 p150 and p60 are highly specific to the H3.1 complex, p48 was present in both complexes (Figure 1B). p48, which was originally identified as retinoblastoma binding protein p48 (RbAp48), copurifies with a variety of chromatin-related complexes, including histone deacetylase and nucleosome-remodeling complexes (Ridgway and Almouzni, 2000), suggesting that p48 could perform a non-CAF-1 function in the H3.3 complex.

Importantly, HIRA was found in the H3.3 complex (Figure 1B). Immunoblotting of the purified complexes revealed that HIRA is highly specific to the H3.3 complex (Figure 1E). HIRA is the human homolog of the *Saccharomyces cerevisiae* proteins Hir1p and Hir2p, which function as cell-cycle-regulated transcriptional repressors of histone genes (Lamour et al., 1995; Lorain et al., 1996). HIRA has recently been identified as a histone chaperone for a DNA-synthesis-independent nucleosome assembly pathway (Ray-Gallet et al., 2002). Our results demonstrate the first link between histone H3.3 and HIRA, suggesting a model for how histone H3.3 could be deposited in a DNA-synthesis-independent manner.

In addition to histone chaperones, HAT1 was identified by mass spectrometric analyses in both the H3.1 and H3.3 complexes (Figure 1B). Newly synthesized histones H3 and H4 are transiently acetylated by HAT1, and then deacetylated shortly after the deposition of the histones into chromosomes (Verreault, 2000). The presence of HAT1 in these complexes supports the link between acetylation and deposition of histones H3 and H4 and supports our hypothesis that histones e-H3.1/e-H3.3 and H4 present in these complexes are predeposited forms.

Both the H3.1 and H3.3 complexes also contain importin 4 (Figure 1B), a recently identified importin β-related receptor that mediates translocation through nuclear pore complexes (Jakel et al., 2002), suggesting that importin 4 plays a role in nuclear transport of the H3.1 and H3.3 complexes.

The H3.1 and H3.3 Complexes Are Involved in Distinct Nucleosome Assembly Pathways

The H3.1 and H3.3 complexes contain distinct histone chaperones: all three subunits of CAF-1, p150, p60, and p48, are associated with H3.1, whereas HIRA is associated with the H3.3 complex (Figure 1). These two chaperones have been shown to be involved in distinct nucleosome assembly pathways in higher eukaryotes. HIRA is critical for a DNA-synthesis-independent nucleosome assembly process (Ray-Gallet et al., 2002), while CAF-1 mediates nucleosome formation coupled to DNA synthesis during DNA replication (Smith and Stillman, 1989) or DNA repair (Gaillard et al., 1996). To analyze the nucleosome assembly activity of the H3.1 and H3.3 complexes in vitro, we used a *Xenopus* egg extract system (HSE) that is highly efficient for nucleosome assembly using either histone deposition pathway (Almouzni and Mechali, 1988; Ray-Gallet and Almouzni, 2004).

Endogenous HIRA or CAF-1 p150 was immunodepleted from HSE, resulting in extracts that were >90% depleted for HIRA or CAF-1 p150 (Figure 2A). These depleted extracts were then used to assay nucleosome assembly on either mock-treated, intact plasmid DNA (p0) to follow nucleosome formation in the absence of DNA synthesis or on UV-treated plasmid DNA (pUV) to follow nucleosome assembly in the presence of DNA synthesis during nucleotide excision repair (NER).

After three hr in the presence of HIRA-depleted extracts, the p0 plasmid was mainly in the relaxed form (Ir) (Figure 2B, lane 2 and Figure 2C top, lane 3), reflecting a defect in nucleosome deposition on DNA not undergoing replication. In contrast, after incubation with mock or CAF-1 p150 depleted extracts, the p0 plasmid was almost fully supercoiled (form I) (Figure 2C top, lanes 2 and 6), showing that both extracts are efficient in promoting nucleosome formation on a template not undergoing DNA synthesis.

With the pUV plasmid the reverse situation was observed. After incubation with CAF-1 p150-depleted extracts, the plasmid remained essentially nucleosome-free (relaxed form Ir) (Figure 2B, lane 5 and Figure 2C bottom, lane 14). However, after incubation with mock- or HIRA-depleted extracts, the repaired plasmid was efficiently assembled into nucleosomes (form I) (Figure 2C bottom, lanes 10 and 11).

In order to attempt to rescue the nucleosome assembly activities of HIRA- and CAF-1 p150-depleted extracts, complementation experiments were carried out with recombinant *Xenopus* HIRA or CAF-1 p150 (Figure 2B, lanes 3 and 6). In both cases the complementation failed, suggesting that the addition of the depleted polypeptide is not sufficient to reconstitute the nucleosome assembly capacities of the depleted HSEs.

The purified H3.1 and H3.3 complexes were tested for their ability to rescue the defect in nucleosome assembly of the depleted extracts. Addition of the H3.3 complex to the HIRA-depleted extracts significantly restored the nucleosome assembly activity of the extract. Indeed, in the presence of the H3.3 complex there is an increase of p0 supercoiled DNA as compared to the HIRA-depleted extract alone (Figure 2C top, compare lanes 3 and 5). In contrast, no change in the p0 plasmid migration was observed when the H3.1 complex was added (Figure 2C top, compare lanes 3 and 4).

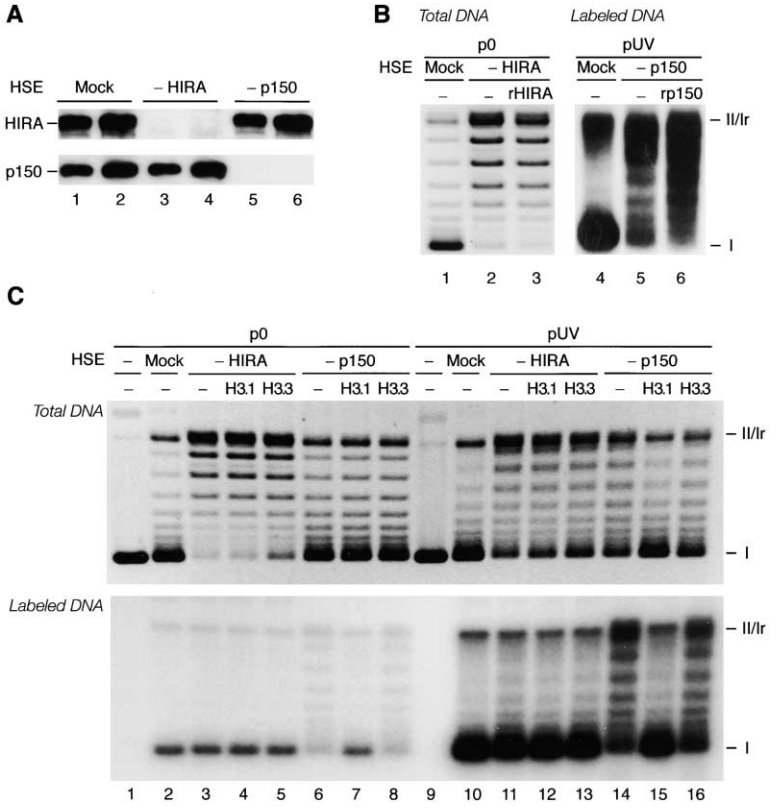

Figure 2. The H3.1 and H3.3 Complexes Mediate DNA-Synthesis-Dependent and -Independent Nucleosome Assembly, Respectively

(A) Immunodepletion of HSEs. Two aliquots (1 and 2 μl; odd and even lanes, respectively) of mock- (lanes 1 and 2), HIRA- (lanes 3 and 4), and CAF-1 p150- (lanes 5 and 6) depleted HSEs were analyzed by immunoblotting with anti-HIRA (top) and anti-CAF-1 p150 (bottom) antibodies.

(B) Recombinant HIRA and CAF-1 p150 are unable to rescue nucleosome assembly activities in immunodepleted HSEs. Nucleosome assembly reactions in the absence of DNA synthesis were carried out with untreated plasmid (p0) in mock- (lane 1) or HIRA-depleted (lanes 2 and 3) HSEs in the absence (lanes 1 and 2) and presence (lane 3) of recombinant HIRA. The DNA products were visualized by ethidium bromide. Nucleosome assembly reactions coupled to DNA repair were carried out with UV-treated plasmid (pUV) in mock- (lane 4) or CAF-1 p150-depleted (lanes 5 and 6) HSEs in the absence (lanes 4 and 5) and presence (lane 6) of recombinant CAF-1 p150. Reactions were performed in the presence of [α-^{32}P]dCTP to follow nucleosome assembly coupled to DNA repair and visualized by autoradiography. The positions of plasmid DNA form I (supercoiled), form II (nicked circular), and form Ir (closed circular) are indicated.

(C) The histone H3.1 and H3.3 complexes mediate DNA-synthesis-dependent and -independent nucleosome assembly, respectively. Nucleosome assembly assays were performed in the presence of [α-^{32}P]dCTP by incubating either mock (lanes 2 and 10), HIRA- (lanes 3∼5 and 11∼13) or p150- (lanes 6∼8 and 14∼16) depleted HSE with either untreated plasmid (p0) (lanes 2∼9) or UV-irradiated plasmid (pUV) (lanes 10∼16). The H3.1 (lanes 4, 7, 12, and 15) or H3.3 (lanes 5, 8, 13, and 16) complexes were added to the reactions to examine their ability to complement nucleosome assembly activities in immunodepleted HSEs. The DNA products were visualized by ethidium bromide (top) and autoradiography (bottom). Input plasmids, p0 (lane 1) and pUV (lane 9), were also analyzed.

Conversely, the nucleosome assembly defect of the CAF-1 p150-depleted extracts was efficiently rescued by the addition of the H3.1 complex to the pUV nucleosome assembly reaction (Figure 2C bottom, compare lanes 14 and 15), whereas the H3.3 complex failed to complement the defect (Figure 2C, bottom, compare lanes 14 and 16). We conclude from these data that the histone H3.1 and H3.3 complexes mediate DNA-synthesis-dependent and DNA-synthesis-independent nucleosomal assembly, respectively.

Histones H3.1 and H3.3 Are Deposited through Distinct Nucleosomal Assembly Pathways

Our data strongly suggest that histones H3.1 and H3.3 are deposited by independent histone chaperone complexes via distinct nucleosomal assembly pathways. To obtain direct evidence that histones H3.1 and H3.3 are indeed assembled by distinct assembly pathways, we performed the following experiments. First, we prepared cytosolic extracts from HeLa cells expressing e-H3.1 or e-H3.3. Immunoblotting data show that these cytosolic extracts contain no detectable CAF-1 or HIRA (Figure 3A), so we employed these extracts as the source of free-tagged histones for nucleosomal assembly reactions. To examine DNA-synthesis-dependent nucleosomal assembly, UV-damaged DNA immobilized onto magnetic beads was incubated with HIRA-depleted HSE in the presence of cytosolic extracts containing e-H3.1 or e-H3.3. These HIRA-depleted extracts are still functional for the CAF-1 dependent pathway as shown in Figure 2. After nucleosomal assembly reactions, histones bound to immobilized DNA were analyzed by immunoblotting. As expected, e-H3.1 was recovered onto immobilized UV-damaged DNA in a CAF-1- (from the HSE) dependent manner (Figure 3B, lanes 2 and 4). In contrast, only the background level of e-H3.3 was detected on the immobilized DNA (lane 8). Taken together with the data in Figure 2, we conclude that histone H3.1, rather than H3.3, is utilized by the DNA-synthesis-dependent nucleosome assembly pathway.

We also examined the deposition of histone H3 in a DNA-synthesis-independent nucleosomal assembly pathway. We used immobilized intact DNA as a template and a CAF-1 p150 depleted HSE in which only the HIRA dependent pathway is functional. In contrast to the DNA-synthesis-dependent deposition, e-H3.3, but not e-H3.1, was recovered onto immobilized intact DNA (Figure 3C, lanes 4 and 8), indicating that histone H3.3 is specifically deposited in DNA-synthesis-independent nucleosome assembly. Taken together, we conclude that histone H3.1 and H3.3 are assembled into nucleosomes via

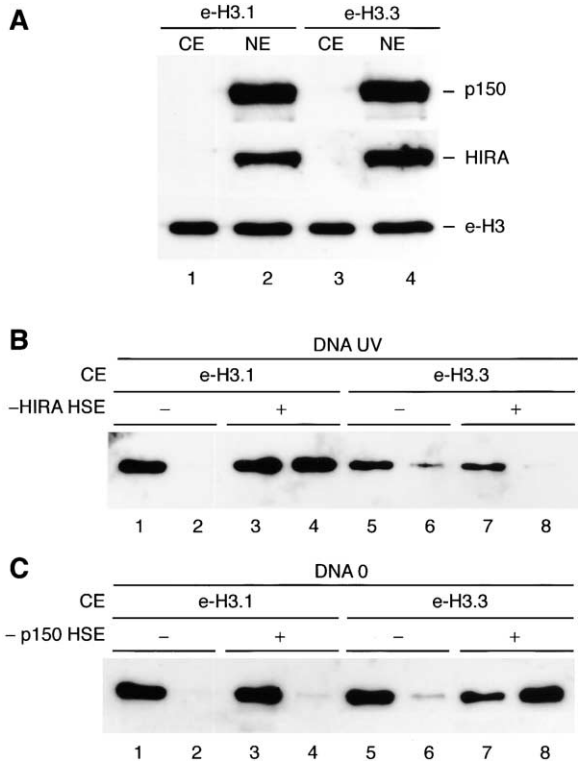

Figure 3. Histones H3.1 and H3.3 Are Specifically Deposited via DNA-Synthesis-Dependent and -Independent Nucleosome Assembly Pathways, Respectively

(A) Cytosolic extracts contain no detectable CAF-1 and HIRA. 20 μg of cytosolic (lanes 1 and 3) and nuclear (lanes 2 and 4) extracts prepared from HeLa cells expressing e-H3.1 (lanes 1 and 2) and e-H3.3 (lanes 3 and 4) were analyzed by immunoblotting with anti-CAF-1 p150 (top), anti-HIRA (middle), and anti-HA (bottom) antibodies.

(B) Histone H3.1 is deposited during DNA-synthesis-dependent nucleosome assembly. Magnetic bead-linked UV-irradiated DNA was incubated with cytosolic extracts containing e-H3.1 (lanes 1∼4) or e-H3.3 (lanes 5∼8) in presence (lanes 3, 4, 7, and 8) or absence (lanes 1, 2, 5, and 6) of HIRA-depleted HSE. 10% input (odd lanes) and bound materials (even lanes) were analyzed by immunoblotting with anti-HA antibody.

(C) Histone H3.3 is deposited during DNA-synthesis-independent nucleosome assembly. Magnetic bead-linked intact DNA was used as in (B) except using incubated with cytosolic extracts containing e-H3.1 (lanes 1∼4) or e-H3.3 (lanes 5∼8) in presence (lanes 3, 4, 7, and 8) or absence (lanes 1, 2, 5, and 6) of CAF-1 p150-depleted HSE. 10% input (odd lanes) and bound materials (even lanes) were analyzed as in (A).

DNA-synthesis-dependent and -independent nucleosome assembly pathways, respectively.

DNA-Synthesis-Dependent Nucleosome Assembly

To determine if a subcomplex is sufficient for the in vitro nucleosome assembly complementation activity, the H3.1 complex purified by FLAG-antibody immunoprecipitation was separated on glycerol gradient by ultracentrifugation. The fractions from glycerol gradient sedimentation were individually purified by HA-antibody immunoprecipitation and analyzed by SDS-PAGE. As shown in Figure 4A, most major polypeptides in the H3.1 complex cosediment in fraction 5, although NASP, CAF-1 p48, and ASF1, which might dissociate from the parental complex, were also detected in fraction 3. CAF-1 p150, p60, and p48, ASF1, NASP, HAT1, and importin 4, as well as e-H3.1 and H4, are found in the fraction 5, consistent with the idea that these factors are stably associated as components of a single complex, or tightly associated subcomplexes that could dynamically exchange.

The fractions collected from the glycerol gradient were pooled as indicated (Figures 4A and 3B), concentrated by HA-antibody immunoprecipitation, and tested for complementation of the nucleosome assembly defect of CAF-1 p150-depleted extracts. As shown in Figure 4D, pools 2 and 3 rescued the defect of CAF-1 p150-depleted extract, and the complementation activity appears to correlate with the amount of CAF-1 in the pools (Figure 4C), as expected.

DNA-Synthesis-Independent Nucleosome Assembly

The histone H3.3 complex was similarly fractionated on a glycerol gradient. Unlike with the H3.1 complex, fractionation of the H3.3 complex gave rise to several subcomplexes (Figure 5A). Immunoblotting of each fraction showed that fractions 15–23, near the bottom of the glycerol gradient, contained HIRA (data not shown). The gradient fractions were pooled, concentrated by HA-antibody immunoprecipitation, and tested for complementation of the nucleosome assembly defect of HIRA-depleted extracts. Immunoblotting of the pooled fractions confirmed that HIRA is specifically found in pool 4 (Figures 5B and 5C). Complementation assays with the pooled fractions revealed that only pool 4 efficiently rescued the deposition defect of HIRA-depleted extracts (Figure 5D).

To gain insight into the mechanisms of DNA-synthesis-independent histone deposition, we further characterized the HIRA-containing H3.3 subcomplex. In the glycerol gradient fractionation, 200 kDa and 150 kDa polypeptides cosedimented with HIRA (Figure 5A). A similar subcomplex, including the 200 kDa and 150 kDa polypeptides, was immunoprecipitated from HeLa nuclear extracts using an anti-HIRA antibody (data not shown), so we conclude that these polypeptides are bona fide subunits of the HIRA-containing H3.3 subcomplex.

The 200 kDa band was found to contain Cabin1, and the 150 kDa band was found to contain ubinuclein, as determined by mass spectrometric analysis (Figures 5A and 5B). Cabin1 has been shown to act as a repressor of the transcription factor MEF2, whose activation by calcium signaling causes apoptosis of T cells (Sun et al., 1998). Activation of calcium signaling leads to dissociation of Cabin1 from MEF2, as a result of the binding of active calmodulin to Cabin1 (Youn et al., 1999). These results suggest that Cabin1 may function in the HIRA-containing H3.3 subcomplex by responding to calcium-signaling pathways. Ubinuclein is a ubiquitously expressed nuclear protein that binds to various transcription factors, including EB1 and c-*jun* (Aho et al., 2000), although the biological roles of ubinuclein remain unclear. In addition to Cabin1 and ubinuclein, ASF1 was found in the HIRA-containing H3.3 subcomplex. Immunoblotting anal-

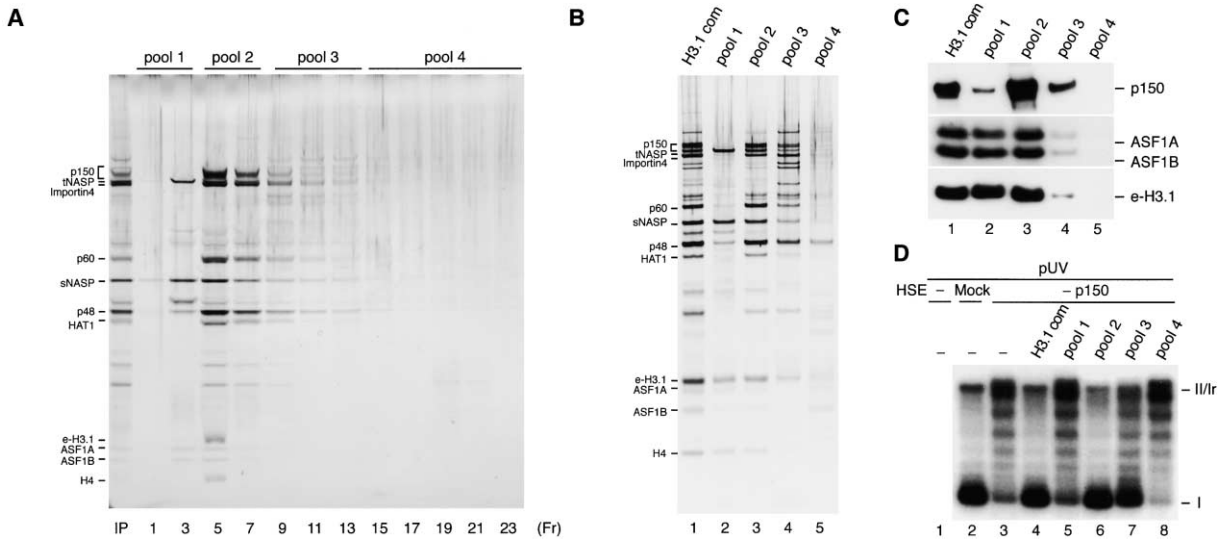

Figure 4. Glycerol Gradient Sedimentation of the H3.1 Complex

(A) Silver staining of the H3.1 complex separated on a glycerol gradient. The H3.1 complex purified by FLAG-antibody immunoprecipitation was separated on a glycerol gradient by ultracentrifugation. Fractions were collected from the top of the gradient, and an aliquot of each fraction (Fr), as well as the input (IP), was immunoprecipitated with anti-HA antibody. The fractions collected from the glycerol gradient were pooled as indicated on the top.

(B) Silver staining of the pooled fractions. Each pool (lanes 2∼5), as well as the input (lane 1), was immunoprecipitated with HA-antibody.

(C) Immunoblotting of the pooled fractions. Each pool (lanes 2∼5), as well as the input (lane 1) was analyzed by immunoblotting with anti-CAF-1 p150 (top), anti-ASF1 (middle), and anti-HA (bottom) antibodies.

(D) Complementation of nucleosome assembly coupled to DNA repair in CAF-1 p150-depleted HSEs. Nucleosome assembly reactions were carried out with pUV in mock- (lane 2) or CAF-1 p150-depleted (lanes 3∼8) HSEs. The H3.1 complex (lane 4) and pooled fractions (lanes 5∼8) were added to determine their ability to complement the nucleosome assembly defect of CAF-1 p150-depleted HSEs. Input plasmid, pUV (lane 1), was also analyzed in parallel.

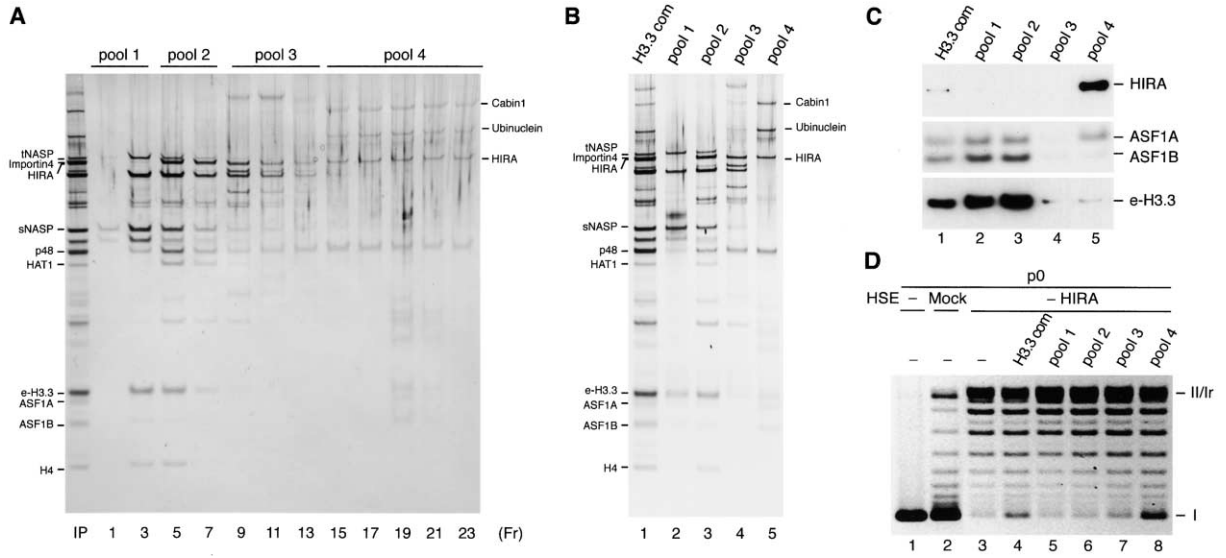

Figure 5. Identification of the HIRA-Containing H3.3 Complex

(A) Glycerol gradient sedimentation of the H3.3 complex. Experiments were performed as in Figure 4A.

(B) Silver staining of the pooled fractions. Experiments were done as in Figure 4B.

(C) Immunoblotting of the pooled fractions. Each pool (lanes 2∼5), as well as the input (lane 1) was analyzed by immunoblotting with anti-HIRA (top), anti-ASF1 (middle), and anti-HA (bottom) antibodies.

(D) Complementation of nucleosome assembly independent of DNA synthesis in HIRA-depleted HSEs. Nucleosome assembly reactions were performed with p0 in mock- (lane 2) or HIRA-depleted (lanes 3∼8) HSEs. The H3.3 complex (lane 4) and pooled fractions (lanes 5∼8) were added as indicated to determine their complementation ability. Input plasmid, p0 (lane 1), was also analyzed in parallel.

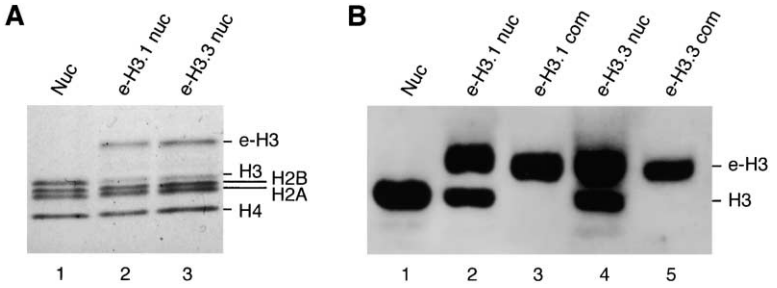

Figure 6. The H3.1 and H3.3 Complexes Possess Only One Molecule of Histone H3

(A) Coomassie blue staining of e-H3.1- and e-H3.3-containing mononucleosomes. e-H3.1- (lane 2) and e-H3.3- (lane 3) containing mononucleosomes purified from nuclear pellets of transduced HeLa cells, as well as control mononucleosomes purified from nontransduced HeLa cells (lane 1) were analyzed by SDS-PAGE.

(B) Immunoblotting of mononucleosomes and deposition complexes. Control mononucleosomes (lane 1), e-H3.1- (lane 2), and e-H3.3- (lane 4) containing mononucleosomes, and the H3.1 (lane 3) and H3.3 (lane 5) complexes were analyzed by immunoblotting with antihistone H3 antibody. The loaded samples were normalized by the amount of histone H4 in a silver-stained gel. The positions for epitope-tagged histone H3 (e-H3.1 or e-H3.3) and native H3 are indicated.

ysis revealed that this complex preferentially contains ASF1A rather than ASF1B (Figure 5C, lane 5). These data suggest that ASF1 proteins may assist nucleosome assembly by HIRA.

Deposition of Histones H3 and H4 as a Dimeric Unit

To obtain further insights into nucleosomal assembly mechanisms of histones H3.1 and H3.3, we purified e-H3.1/e-H3.3-containing mononucleosomes from nuclear pellets. The nuclear pellets prepared from e-H3.1/e-H3.3-expressing cells were homogenized with a dounce grinder to solubilize chromatin. After micrococcal nuclease digestion, e-H3.1/e-H3.3-containing nucleosomes were purified by anti-FLAG antibody immunoprecipitation. The resulting material was contaminated with $<5\%$ dinucleosomes and was further purified by glycerol gradient centrifugation, yielding e-H3.1/e-H3.3–containing mononucleosomes at $>99\%$ purity, as estimated from the analysis of a SYBR green-stained DNA gel (data not shown).

The Coomassie blue-stained SDS-PAGE gel showed that these mononucleosomes contain e-H3.1/e-H3.3, untagged histone H3, H2A, H2B, and H4 at an approximate ratio of 1:1:2:2:2 (Figure 6A). Note that although the intensity of the epitope-tagged H3 appears to be higher than that of untagged H3, this could be due to the higher sensitivity of the epitope-tagged H3 to Coomassie blue staining. The presence of untagged H3 and the lower representation of e-H3.1 and e-H3.3 compared to native histones H2A, H2B, and H4 are consistent with the expression levels of e-H3.1 and e-H3.3 in the transduced cells relative to endogenous H3.1 and H3.3 ($<10\%$ of endogenous H3.1 and H3.3, respectively; data not shown). However, surprisingly, in the purified e-H3.1/e-H3.3 predeposition complexes, untagged histone H3 was not detected by silver staining or mass spectrometric analyses (Figure 1B). Consistent with these results, untagged H3 was not detected in these complexes by immunoblotting with antihistone H3 antibody (Figure 6B). Given that untagged H3 is far more abundant than epitope-tagged H3, if histones H3–H4 in the predeposition complexes are tetramers, untagged H3 should be detected in the complexes. Nevertheless, untagged histone H3 was not detected in the predeposition complexes, leading us to conclude that the H3.1/H3.3 predeposition complex includes an e-H3.1/e-H3.3–H4 heterodimer, rather than a heterotetramer.

The critical question becomes whether H3.1–H4 and H3.3–H4 dimers are randomly deposited, resulting in the presence of both types of dimers in a single mononucleosome, or whether mononucleosomes are uniform in their H3 composition. To address this question, we analyzed the untagged histone H3 in the e-H3.1- and e-H3.3-containing mononucleosomes (the bands labeled as H3 in Figures 6A) by mass spectrometry. Semiquantitative analyses of tryptic peptides specific to histones H3.1 and H3.3 revealed that there was no detectable histone H3.3 ($<0.1\%$ of H3.1) in e-H3.1-containing mononucleosomes. Similarly, only a negligible amount of histone H3.1 (0.5% of H3.3) was found in e-H3.3-containing mononucleosomes. These results suggest that histones H3.1 and H3.3 are homogenously deposited in mononucleosomes, consistent with our data that histones H3.1 and H3.3 are deposited via distinct nucleosome assembly pathways in vitro (Figure 3).

Discussion

Mechanisms of Nucleosome Assembly

Various experimental results, both in vitro and in vivo, have culminated in the conclusion that nucleosome core particles are assembled in two steps (reviewed in Wolffe, 1998). First, a tetramer of histones H3 and H4, $(H3–H4)_2$, is deposited on DNA, organizing the central 120 base pairs of DNA identically to that found in the nucleosome. Subsequently, two H2A–H2B dimers associate with the deposited $(H3–H4)_2$, completing formation of a nucleosome core particle and organizing 146 base pairs of DNA. Based on the observation that histones H3 and H4 exist as a stable $(H3–H4)_2$ tetramer in solution in the absence of DNA (Baxevanis et al., 1991), it was hypothesized that histones H3 and H4 are deposited as a tetrameric unit in vivo. In contrast, we show that in predeposited form, histones H3 and H4 exist as a heterodimer, not as a heterotetramer, in both the H3.1 and H3.3 complexes. Accordingly, we predict that histones H3 and H4 are deposited on DNA as a dimeric unit.

If our prediction is true, then a crucial question becomes from where do the remaining H3–H4 molecules come to complete the $(H3–H4)_2$ tetramer on DNA? It is possible that two H3.1 (or H3.3) complexes deposit their H3–H4 dimers onto DNA strands simultaneously to assemble a $(H3–H4)_2$ tetramer (Figure 7A, left). This would perhaps explain the dimerization properties of CAF-1 p150 (Quivy et al., 2001), which is critical for its function.

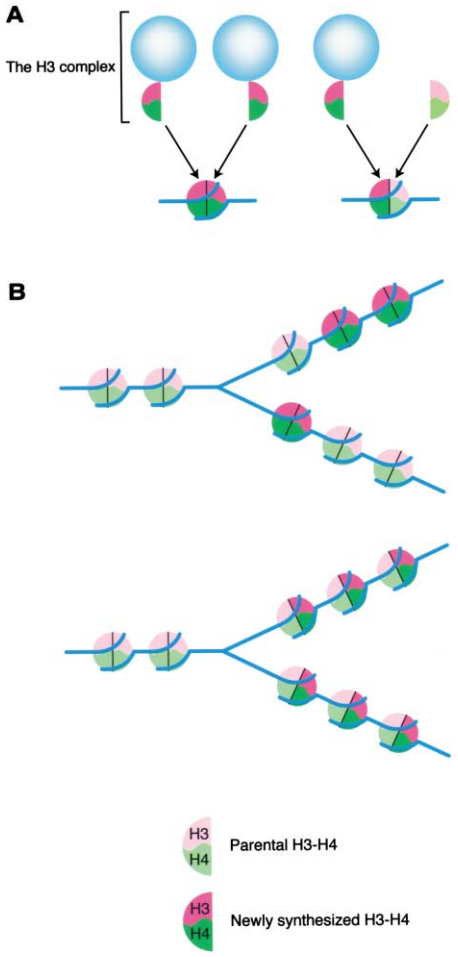

Figure 7. Possible Mechanisms for Nucleosomal Assembly

(A) Models for nucleosomal assembly. Given that the H3.1/H3.3 complex contains only a H3–H4 dimer, deposition of an additional H3–H4 dimer would be required for formation of the $(H3–H4)_2$ tetramer on DNA. (Left) One possibility is that two H3.1/H3.3 complexes deposit their H3–H4 dimers simultaneously to assemble a $(H3–H4)_2$ tetramer. (Right) An alternative possibility is that a single H3.1/H3.3 complex deposits its H3–H4 dimer, together with a free H3–H4 dimer, possibly coming from parental nucleosomes.

(B) Models for chromatin replication. (Top) The tetrameric model: parental $(H3–H4)_2$ tetramers are dissociated from nucleosomes and deposited onto one of the daughter DNA strands stochastically. Newly synthesized $(H3–H4)_2$ tetramers are deposited on the daughter DNA strands in a CAF-1-dependent manner. In this model, parental and newly synthesized $(H3–H4)_2$ tetramers are deposited into distinct nucleosomes. (Bottom) The dimeric model: parental $(H3–H4)_2$ tetramers are dissociated into H3–H4 dimers and are paired with newly synthesized H3–H4 dimers on each daughter DNA strand by the action of the H3.1 deposition complex. In this model, H3–H4 dimers from parental nucleosomes are segregated evenly onto daughter DNA strands.

Alternatively, another likely possibility is that a single complex deposits its H3–H4 dimer, together with either a free H3–H4 dimer or a H3–H4 dimer from another source (Figure 7A, right). In this context, the presence of two chaperones for histones H3–H4, CAF-1, and ASF1 (or HIRA and ASF1) in the H3.1 (or H3.3) complex, may be a key issue. Although ASF1 and CAF-1 have been shown to independently interact with histones H3 and H4 (Verreault et al., 1996; Tyler et al., 1999), it is yet unclear if a H3–H4 dimer associates directly with ASF1 or CAF-1 in the H3.1 complex. However, since both chaperones are present, a given H3.1 complex could potentially bind H3–H4 dimers through each histone chaperone and deposit two H3–H4 dimers simultaneously to form the $(H3–H4)_2$ tetramer on DNA. While the recruitment of a free H3–H4 dimer might be an intermediate step for nucleosome formation, this intermediate complex would be very unstable since we did not detect a second H3–H4 dimer in the purified complex (Figure 6).

A similar mechanism might be involved in nucleosomal assembly by the HIRA-containing H3.3 subcomplex, i.e., ASF1 and HIRA may each hold a H3–H4 dimer and cooperatively deposit the two dimers into a single nucleosome. However, a significant difference compared to the H3.1 complex is that the HIRA-containing complex mediates DNA-synthesis-independent nucleosome assembly. In DNA-synthesis-dependent nucleosome assembly, the H3.1 complex appears to be recruited near target sites via interaction of CAF-1 with PCNA (Shibahara and Stillman, 1999; Moggs et al., 2000), while it is unknown how the assembly machinery is targeted in the DNA-synthesis-independent pathway. One possibility is that histone H3.3 is preferentially deposited in transcriptionally active loci, marking active chromatin (Vermaak et al., 2003). In this context, ubinuclein in the complex may play a role in targeting active chromatin through its interaction with various transcription factors (Aho et al., 2000). We have demonstrated that histone H3.3 belongs to several subcomplexes in addition to the HIRA-containing subcomplex (Figure 4), suggesting that histone H3.3 may be assembled to different loci via distinct pathways.

Semiconservative Model for Nucleosomal Assembly

Chromatin is a heterogeneous and diverse array that contains epigenetic information, encoded by histone modifications, nucleosomal positions, and histone variants (Turner, 2000; Jenuwein and Allis, 2001). Although some epigenetic information could be maintained after DNA replication or nucleotide excision repair, the mechanisms for this maintenance remain unclear. Here, we propose a semiconservative model for nucleosomal assembly.

According to the well-accepted model, newly replicated DNA is assembled into chromatin using parental histones or de novo synthesized histones in separate pathways (Figure 7B, top) (reviewed in Wolffe, 1998). The first pathway involves transfer of the parental $(H3–H4)_2$ tetramers onto one of the daughter DNA strands. Each parental nucleosome is postulated to be transiently disrupted into a $(H3–H4)_2$ tetramer and two H2A-H2B dimers during passage of the replication fork (Gruss et al., 1993). Subsequently, each parental $(H3–H4)_2$ tetramer is segregated randomly onto either of the daughter DNA strands by unknown mechanisms (Cusick et al., 1984; Sogo et al., 1986; Burhans et al., 1991). The second pathway involves deposition of newly synthesized $(H3–H4)_2$ tetramers on daughter DNA strands in a CAF-1-dependent manner (Kaufman and Almouzni, 2000; Verreault, 2000; Krude and Keller, 2001). By this model, old parental histones and newly synthesized histones are deposited

into distinct nucleosomes. If two H3 complexes deposit their H3–H4 dimers to assemble nucleosomes, this model would be supported by our data.

We propose an alternative model in which parental $(H3–H4)_2$ tetramers are disrupted and segregated evenly onto daughter DNA strands as H3–H4 dimers, which are then paired with newly synthesized H3–H4 dimers by the action of the H3.1 complex (Figure 7B, bottom). By this model, the leading and lagging strands of replicating DNA would each bind a H3.1 complex, trap a parental H3–H4 dimer, and deposit the two H3–H4 dimers onto daughter DNA strands to complete the tetramer. This model allows deposition of mixed parental and de novo-synthesized histones in the same nucleosome particle, ensuring inheritance of parental H3–H4 dimers in all nucleosome core particles formed on newly synthesized DNA strands. Considering that we find only mononucleosomes homogeneous in their H3 composition, the existence of mixed H3.3/H3.1 mononucleosomes can only be transient or nonexistent. We can speculate that when duplication occurs in H3.3-containing nucleosomes, a CAF-1 pathway first deposits an H3.1–H4 dimer, together with a parental H3.3–H4 dimer, and H3.1 is replaced with H3.3 by HIRA in a postreplicative pathway. Alternatively, it is possible that an uncharacterized H3.3 subcomplex plays a role in duplication of H3.3-containing nucleosomes. Future experiments will address this issue.

The semiconservative model can also be applied to nucleosome assembly coupled to NER. To overcome the inhibition imposed by nucleosomal structure, damaged nucleosomes are thought to be temporally disrupted, permitting access of NER machinery to DNA lesions. During NER, CAF-1 appears to target the repair site by interacting with PCNA (Shibahara and Stillman, 1999; Moggs et al., 2000; Green and Almouzni, 2003), and allowing for the rebuilding of nucleosomes on the repaired DNA. Based on our data, we propose that the H3.1 complex, recruited near DNA lesions through CAF-1 interaction with PCNA, traps an H3–H4 dimer from damaged nucleosomes. The H3.1 complex would then deposit this dimer rescued from the original nucleosome with one newly synthesized dimer on the repaired DNA. This mechanism would allow for the preservation of an original H3–H4 dimer, with its epigenetic information, after NER. Our semiconservative histone deposition model, allowing deposition of mixed parental and de novo synthesized histones in the same nucleosome particle, provides new insights into possible mechanisms for maintenance and transmission of epigenetic information to nascent chromatin after DNA replication as well as after NER.

Experimental Procedures

Purification of the H3.1 and H3.3 Complexes

The H3.1 and H3.3 complexes were purified from nuclear extracts prepared from HeLa cells expressing the H3.1 or H3.3 proteins fused with C-terminal FLAG- and HA-epitope tags (e-H3.1/e-H3.3) by immunoprecipitation on anti-FLAG antibody-conjugated agarose. The bound polypeptides were eluted with the FLAG peptide and were further affinity purified by anti-HA antibody-conjugated agarose as described (Nakatani and Ogryzko, 2004). For density gradient sedimentation, 0.5 ml of the FLAG peptide-eluted material was loaded onto a 4 ml glycerol gradient (10%–40%) and spun at 368,000 × g in a Beckman SW55Ti rotor for 2 hr. 200 μl fractions were collected from the top of the gradient using a fractionator (model 184; Brandel, Maryland) connected to a fraction collector (model 2128; Bio-Rad, California). H3.1 or H3.3 complexes were immunoprecipitated from individual or pooled fractions with anti-HA antibody-conjugated agarose and eluted with HA peptide.

Purification of Mononucleosomes Containing e-H3.1 or e-H3.3

Oligonucleosome fragments were prepared from the nuclear pellets and digested with micrococcal nuclease as described (Utley et al., 1996). Nucleosomes containing e-H3.1 or e-H3.3 were purified from the resulting material by immunoprecipitation with anti-FLAG antibody and eluted with FLAG peptide as described (Nakatani and Ogryzko, 2004). After glycerol gradient centrifugation of the immunopurified materials, fractions containing pure mononucleosomes were pooled.

Immunofluorescence Microscopy

Cells were fixed by incubating in 3% paraformaldehyde for 5 min at room temperature, followed by methanol, cooled at −20°C for 5 min. Then cells were treated with rabbit polyclonal HA-antibody (Covance Inc., NJ) in TBST (20 mM Tris-HCl buffer, [pH 8.0], 150 mM NaCl, 0.5% Triton X-100) containing 5% calf serum for 1 hr followed by three washes and incubation with Alexa488-conjugated antirabbit IgG antibody (Molecular Probe) for 1 hr. After being washed with TBST three times, cells were stained with DAPI and examined using DeltaVision deconvolution microscope.

Mass Spectrometry

Protein bands were cut out from SDS-PAGE gels, digested with trypsin in situ, and analyzed by MALDI-TOF mass spectrometry and/or by microcapillary LC-MS with automated switching to MS/MS mode for peptide fragmentation and sequence analysis (Gygi et al., 1999). For mass spectrometric analyses of histones H3.1 and H3.3, only the m/z of the doubly charged peptides SAPATGGVK (m/z = 394.2) and SAPSTGGVK (m/z = 402.2), specific to H3.1 and H3.3, respectively, were selectively analyzed. To gain better selectivity, MS^3 fragmentation was performed on an ion trap mass spectrometer. The mass spectrometer was programmed to do fragmentation on the peak within the MS/MS (MS^2) fragmentation to produce an MS^3 fragmentation pattern. Peptides were identified from the fragmentation pattern of the ms/ms and the ms^3 data. To determine the ratio between H3.1 and H3.3, the peaks corresponding to the above mentioned peptides were compared based on the assumption that both peptides have similar response factors, since they only differ by one amino acid.

Nucleosome Assembly Assay

High-speed egg extracts (HSEs) were prepared as described (Almouzni, 1998). For immunodepletion of the HSEs, antibodies against *Xenopus* HIRA (Ray-Gallet et al., 2002) and *Xenopus* CAF-1 p150 (Quivy et al., 2001) were conjugated to protein A Sepharose (Amersham Biosciences) and were incubated with HSEs for 1.5 hr at 4°C. As templates for nucleosome assembly reactions, pBS plasmid with no lesion induced (p0) was used for DNA-synthesis-independent nucleosome assembly, while UV-irradiated (500 J/m^2) pBS (pUV) was used for DNA-synthesis-dependent nucleosome assembly. The reaction mixture consisted of 10 μl HSE (depleted or mock-depleted) and 15 μl p0 or pUV (150 ng) in a reaction buffer containing 5 mM $MgCl_2$, 40 mM HEPES-KOH, [pH 7.8], 0.5 mM DTT, 4 mM ATP, 40 mM phosphocreatine, 2.5 μg of creatine phosphokinase, and 5 μCi [α-^{32}P]dCTP, and the reaction was carried out for 3 hr at 23°C (Gaillard et al., 1999; Ray-Gallet and Almouzni, 2004). The purified plasmid DNA was subjected to agarose gel electrophoresis and analyzed by staining with ethidium bromide (to assess topological changes in total DNA) and by autoradiography (to detect labeled repaired DNA).

Immobilized DNA templates was carried out as previously described (Moggs et al., 2000). To obtain the epitope-tagged histones, cytosolic extracts from HeLa cells expressing either e-H3.1 or e-H3.3 were prepared as described (Martini et al., 1998). Magnetic bead-linked UV-irradiated or intact DNA (150 ng) was incubated with either e-H3.1 or e-H3.3 cytosolic extracts (30 μg) in presence of HIRA-

depleted or CAF-1-depleted HSE (8 μl). After 3 hr incubation at room temperature, the bead-linked DNA was washed 3 times in a washing buffer containing 40 mM HEPES-KOH, [pH 7.8], 300 mM KCl and 0.5% NP40, and resuspended in Laemmli buffer.

Antibodies

Antibodies employed are as follows: anti-p150 antibody (H300; Santa Cruz Biotechnology, Inc.); anti-HIRA (WC15 and WC119) (Hall et al., 2001); anti-ASF1 (D.B.K. and G.A., unpublished data) (Sillje and Nigg, 2001); antihistone H3 (C-16; Santa Cruz Biotechnology, Inc.); antihistone H2A (14–493; Upstate Group, Inc.); and histone H2B (14–491) (Upstate Group, Inc.).

Acknowledgments

We would like to thank Steven Gygi and Ross Tamaino in the Taplin Biological Mass Spectrometry Facility; Junichi Sawada for microscopic analysis; Kami Ahmad for useful comments; and Deborah Goff for editing the manuscript. This work was supported, in part, by grants from NIH (GM065939-02) and Human Frontier Science Program to Y.N.; and by grants from la Ligue Nationale contre le Cancer (Equipe Labelisée la Ligue), Euratom (FIGH-CT1999-00010), the Commissariat à l'Energie Atomique (LRC no. 26), and a Program Incitatif et Collaboratif from the Curie Institute on epigenetic parameters to G.A. H.T. was supported by a JSPS Postdoctoral Fellowship for Research Abroad.

Received: September 17, 2003
Revised: December 16, 2003
Accepted: December 17, 2003
Published: January 8, 2004

References

Ahmad, K., and Henikoff, S. (2002). The histone variant H3.3 marks active chromatin by replication-independent nucleosome assembly. Mol. Cell *9*, 1191–1200.

Aho, S., Buisson, M., Pajunen, T., Ryoo, Y.W., Giot, J.F., Gruffat, H., Sergeant, A., and Uitto, J. (2000). Ubinuclein, a novel nuclear protein interacting with cellular and viral transcription factors. J. Cell Biol. *148*, 1165–1176.

Alekseev, O.M., Bencic, D.C., Richardson, R.T., Widgren, E.E., and O'Rand, M.G. (2003). Overexpression of the linker histone-binding protein tNASP affects progression through the cell cycle. J. Biol. Chem. *278*, 8846–8852.

Almouzni, G. (1998). Assembly of chromatin and nuclear structures in Xenopus egg extracts. In Chromatin, A Practical Approach (London: Oxford University Press), pp. 195–218.

Almouzni, G., and Mechali, M. (1988). Assembly of spaced chromatin promoted by DNA synthesis in extracts from Xenopus eggs. EMBO J. *7*, 665–672.

Baxevanis, A.D., and Landsman, D. (1998). Histone sequence database: new histone fold family members. Nucleic Acids Res. *26*, 372–375.

Baxevanis, A.D., Godfrey, J.E., and Moudrianakis, E.N. (1991). Associative behavior of the histone (H3–H4)2 tetramer: dependence on ionic environment. Biochemistry (Mosc.) *30*, 8817–8823.

Brown, D.T., Wellman, S.E., and Sittman, D.B. (1985). Changes in the levels of three different classes of histone mRNA during murine erythroleukemia cell differentiation. Mol. Cell. Biol. *5*, 2879–2886.

Burhans, W.C., Vassilev, L.T., Wu, J., Sogo, J.M., Nallaseth, F.S., and DePamphilis, M.L. (1991). Emetine allows identification of origins of mammalian DNA replication by imbalanced DNA synthesis, not through conservative nucleosome segregation. EMBO J. *10*, 4351–4360.

Cusick, M.E., DePamphilis, M.L., and Wassarman, P.M. (1984). Dispersive segregation of nucleosomes during replication of simian virus 40 chromosomes. J. Mol. Biol. *178*, 249–271.

Franklin, S.G., and Zweidler, A. (1977). Non-allelic variants of histones 2a, 2b and 3 in mammals. Nature *266*, 273–275.

Gaillard, P.H., Martini, E.M., Kaufman, P.D., Stillman, B., Moustacchi, E., and Almouzni, G. (1996). Chromatin assembly coupled to DNA repair: a new role for chromatin assembly factor I. Cell *86*, 887–896.

Gaillard, P.H., Roche, D., and Almouzni, G. (1999). Nucleotide excision repair coupled to chromatin assembly. In Methods of Mol. Biol., P.B. Becker, ed. (Totowa, NJ: Humana Press), pp. 231–243.

Green, C.M., and Almouzni, G. (2003). Local action of the chromatin assembly factor CAF-1 at sites of nucleotide excision repair in vivo. EMBO J., *22*, 5163–5174.

Groisman, R., Polanowska, J., Kuraoka, I., Sawada, J., Saijo, M., Drapkin, R., Kisselev, A.F., Tanaka, K., and Nakatani, Y. (2003). The ubiquitin ligase activity in the DDB2 and CSA complexes is differentially regulated by the COP9 signalosome in response to DNA damage. Cell *113*, 357–367.

Gruss, C., Wu, J., Koller, T., and Sogo, J.M. (1993). Disruption of the nucleosomes at the replication fork. EMBO J. *12*, 4533–4545.

Gygi, S.P., Rochon, Y., Franza, B.R., and Aebersold, R. (1999). Correlation between protein and mRNA abundance in yeast. Mol. Cell. Biol. *19*, 1720–1730.

Hall, C., Nelson, D.M., Ye, X., Baker, K., DeCaprio, J.A., Seeholzer, S., Lipinski, M., and Adams, P.D. (2001). HIRA, the human homologue of yeast Hir1p and Hir2p, is a novel cyclin-cdk2 substrate whose expression blocks S-phase progression. Mol. Cell. Biol. *21*, 1854–1865.

Ikura, T., Ogryzko, V.V., Grigoriev, M., Groisman, R., Wang, J., Horikoshi, M., Scully, R., Qin, J., and Nakatani, Y. (2000). Involvement of the TIP60 histone acetylase complex in DNA repair and apoptosis. Cell *102*, 463–473.

Jakel, S., Mingot, J.M., Schwarzmaier, P., Hartmann, E., and Gorlich, D. (2002). Importins fulfil a dual function as nuclear import receptors and cytoplasmic chaperones for exposed basic domains. EMBO J. *21*, 377–386.

Jenuwein, T., and Allis, C.D. (2001). Translating the histone code. Science *293*, 1074–1080.

Kaufman, P.D., and Almouzni, G. (2000). DNA replication, nucleotide excision repair and nucleosome assembly. In Chromatin Structure and Gene Expression, S.C.R. Elgin, and J.L. Workman, eds. (London: Oxford University Press), pp. 24–48.

Krude, T., and Keller, C. (2001). Chromatin assembly during S phase: contributions from histone deposition, DNA replication and the cell division cycle. Cell. Mol. Life Sci. *58*, 665–672.

Lamour, V., Lecluse, Y., Desmaze, C., Spector, M., Bodescot, M., Aurias, A., Osley, M.A., and Lipinski, M. (1995). A human homolog of the S. cerevisiae HIR1 and HIR2 transcriptional repressors cloned from the DiGeorge syndrome critical region. Hum. Mol. Genet. *4*, 791–799.

Lorain, S., Demczuk, S., Lamour, V., Toth, S., Aurias, A., Roe, B.A., and Lipinski, M. (1996). Structural organization of the WD repeat protein-encoding gene HIRA in the DiGeorge syndrome critical region of human chromosome 22. Genome Res. *6*, 43–50.

Martini, E., Roche, D.M., Marheineke, K., Verreault, A., and Almouzni, G. (1998). Recruitment of phosphorylated chromatin assembly factor 1 to chromatin after UV irradiation of human cells. J. Cell Biol. *143*, 563–575.

Mello, J.A., Sillje, H.H., Roche, D.M., Kirschner, D.B., Nigg, E.A., and Almouzni, G. (2002). Human Asf1 and CAF-1 interact and synergize in a repair-coupled nucleosome assembly pathway. EMBO Rep. *3*, 329–334.

Moggs, J.G., Grandi, P., Quivy, J.P., Jonsson, Z.O., Hubscher, U., Becker, P.B., and Almouzni, G. (2000). A CAF-1-PCNA-mediated chromatin assembly pathway triggered by sensing DNA damage. Mol. Cell. Biol. *20*, 1206–1218.

Nakatani, Y., and Ogryzko, V.V. (2004). Immuno-affinity purification of mammalian protein complexes. Methods Enzymol. *370*, in press.

Ogawa, H., Ishiguro, K., Gaubatz, S., Livingston, D.M., and Nakatani, Y. (2002). A complex with chromatin modifiers that occupies E2F- and Myc-responsive genes in G0 cells. Science *296*, 1132–1136.

Quivy, J.P., Grandi, P., and Almouzni, G. (2001). Dimerization of the largest subunit of chromatin assembly factor 1: importance in vitro and during Xenopus early development. EMBO J. *20*, 2015–2027.

Ray-Gallet, D., and Almouzni, G. (2004). DNA synthesis-dependent and -independent chromatin assembly pathways in Xenopus egg extracts. Methods Enzymol. *375*, in press.

Ray-Gallet, D., Quivy, J.P., Scamps, C., Martini, E.M., Lipinski, M., and Almouzni, G. (2002). HIRA is critical for a nucleosome assembly pathway independent of DNA synthesis. Mol. Cell *9*, 1091–1100.

Richardson, R.T., Batova, I.N., Widgren, E.E., Zheng, L.X., Whitfield, M., Marzluff, W.F., and O'Rand, M.G. (2000). Characterization of the histone H1-binding protein, NASP, as a cell cycle-regulated somatic protein. J. Biol. Chem. *275*, 30378–30386.

Ridgway, P., and Almouzni, G. (2000). CAF-1 and the inheritance of chromatin states: at the crossroads of DNA replication and repair. J. Cell Sci. *113*, 2647–2658.

Shibahara, K., and Stillman, B. (1999). Replication-dependent marking of DNA by PCNA facilitates CAF-1-coupled inheritance of chromatin. Cell *96*, 575–585.

Sillje, H.H., and Nigg, E.A. (2001). Identification of human Asf1 chromatin assembly factors as substrates of tousled-like kinases. Curr. Biol. *11*, 1068–1073.

Smith, S., and Stillman, B. (1989). Purification and characterization of CAF-I, a human cell factor required for chromatin assembly during DNA replication in vitro. Cell *58*, 15–25.

Sogo, J.M., Stahl, H., Koller, T., and Knippers, R. (1986). Structure of replicating simian virus 40 minichromosomes. The replication fork, core histone segregation and terminal structures. J. Mol. Biol. *189*, 189–204.

Sun, L., Youn, H.D., Loh, C., Stolow, M., He, W., and Liu, J.O. (1998). Cabin *1*, a negative regulator for calcineurin signaling in T lymphocytes. Immunity *8*, 703–711.

Turner, B.M. (2000). Histone acetylation and an epigenetic code. Bioessays *22*, 836–845.

Tyler, J.K., Adams, C.R., Chen, S.R., Kobayashi, R., Kamakaka, R.T., and Kadonaga, J.T. (1999). The RCAF complex mediates chromatin assembly during DNA replication and repair. Nature *402*, 555–560.

Tyler, J.K., Collins, K.A., Prasad-Sinha, J., Amiott, E., Bulger, M., Harte, P.J., Kobayashi, R., and Kadonaga, J.T. (2001). Interaction between the Drosophila CAF-1 and ASF1 chromatin assembly factors. Mol. Cell. Biol. *21*, 6574–6584.

Utley, R.T., Owen-Hughes, T.A., Juan, L.-J., Cote, J., Adams, C.C., and Workman, J.L. (1996). In vitro analysis of transcription factor binding to nucleosomes and nucleosome disruption/displacement. Methods Enzymol. *274*, 276–291.

Vermaak, D., Ahmad, K., and Henikoff, S. (2003). Maintenance of chromatin states: an open-and-shut case. Curr. Opin. Cell Biol. *15*, 266–274.

Verreault, A. (2000). De novo nucleosome assembly: new pieces in an old puzzle. Genes Dev. *14*, 1430–1438.

Verreault, A., Kaufman, P.D., Kobayashi, R., and Stillman, B. (1996). Nucleosome assembly by a complex of CAF-1 and acetylated histones H3/H4. Cell *87*, 95–104.

Wolffe, A. (1998). Chromatin: Structure and Function. 3rd ed. (London: Academic Press).

Wu, R.S., Tsai, S., and Bonner, W.M. (1982). Patterns of histone variant synthesis can distinguish G0 from G1 cells. Cell *31*, 367–374.

Wunsch, A.M., and Lough, J. (1987). Modulation of histone H3 variant synthesis during the myoblast-myotube transition of chicken myogenesis. Dev. Biol. *119*, 94–99.

Youn, H.D., Sun, L., Prywes, R., and Liu, J.O. (1999). Apoptosis of T cells mediated by Ca2+-induced release of the transcription factor MEF2. Science *286*, 790–793.

Zweidler, A. (1984). Core histone variants of the mouse: primary structure and differential expression. In Histone Genes, Structure, Organization, and Regulation, G.S. Stein, J.L. Stein, and W.F. Marzluff, eds. (New York: John Wiley & Sons).